Available Online

JOURNAL OF SCIENTIFIC RESEARCH

J. Sci. Res. **14** (1), 79-89 (2022)

www.banglajol.info/index.php/JSR

Structure, Vibrational Analysis and Chemical Reactivity Descriptors of 4-Bromo-3-(Methoxymethoxy) Benzoic Acid: A DFT Study

S. Yadav[1], A. Khare[1], K, K. Yadav[1], P. C. Maurya[1], A. K. Singh[2], A. Kumar[1*]

[1]Department of Physics, University of Lucknow, Lucknow-226007, India

[2]Department of Chemistry, University of Lucknow, Lucknow-226007, India

Received 29 May 2021, accepted in final revised form 16 October 2021

Abstract

In this study, the structure and various molecular parameters of 4-bromo-3-(methoxymethoxy) benzoic acid are determined at the B3LYP/6-311++G(d,p) level of theory. Present study provides comparision and discussion of calculated and experimental optimized parameters. The values of descriptors such as ionization energy, hardness, electrophilicity, condensed Fukui function and energy were determined to predict the reactivity of 4-bromo-3-(methoxymethoxy) benzoic acid. The influence of the solvent on reactivity parameters has been studied adopting the PCM model. The analysis shows that solvation alters the values of reactivity descriptors. A vibrational assessment of the molecule has also been performed. To gain a better understanding of the properties of the title molecule, parameters such as the molecular electrostatic potential surface and the HOMO-LUMO band gap have been computed. The dipole moment, polarizability and hyperpolarizability were also estimated to probe into non-linear optical properties of the chemical.

Keywords: Vibrational analysis; Reactivity; Fukui functions.

doi: http://dx.doi.org/10.3329/jsr.v14i1.53339 J. Sci. Res. **14** (1), 79-89 (2022)

1. Introduction

In this study the compound 4-bromo-3-(methoxymethoxy) benzoic acid (MBMMBA) which is derivative of bromo–hydroxy–benzoic acids is considered. A diverse range of biological properties such as antitumor, antiviral, antifungal, and antimitotic effects have been reported for ester derivatives [1,2]. These compounds have also been tested to act as antiproliferative agent [3]. Azo-ester bridged compounds were studied for enantiotropic liquid crystalline mesophase character and optical activity [4]. Molecular modelling studies revealed that many derivatives were well tolerated at the interface between ARF1 and its guanine nucleotide exchange factor ARNO. Fluorescence imaging assays confirmed the Golgi-disruptive properties of the ester derivatives [5]. Murthy *et al.* [6] recently described synthesis and crystal structure of the title compound. Keeping the above mentioned important properties and applications of ester derivatives in mind, the

* *Corresponding author:* akgkp25@yahoo.co.in

outcomes from DFT/B3LYP analyses of various properties of MBMMBA are presented here. This study on the MBMMBA included the optimization of equilibrium geometry as well as the estimation of ground state characteristics at the DFT/6-311++G (d, p) level. Theoretical infrared spectra are generated, and normal mode analysis of the identified compound is also completed. The vibrational evaluation carries comprehensive data about the intermolecular vibrations. The quantitative structure - activity association based on an analysis of the frontier orbital gap, dipole moment data, and the MBMMBA molecule's molecular electrostatic potential map were used to observe the active sites of the chemical compound. The efficacy of bioactivity of drug in pharmaceutical applications is strongly correlated with solvation phases [7,8]. So, local reactivity parameters have also been calculated for the title compound and effect of solvation on these parameters has been studied. The non linear optical parameters such as polarizability and first static hyperpolarizability of title compound have also been discussed elaborately. To the best of our knowledge, this type of study on the title compound has been done first time.

2. Materials and Methods

The DFT calculations [9] have been excecuted with the G09 software [10], Becke's three parameter hybrid exchange functionals [11] and Lee–Yang–Parr correlation functionals (B3LYP) in the current communication [12,13] . The basis set 6-311++G(d, p) was used in particular because of its advantage in performing faster calculations with comparatively high precision [14,15]. The measured frequencies are scaled down by the necessary factor [16,17] to incorporate anharmonicity. MEPS was generated and displayed using Gaussview-5 [18] at the above mentioned theory. The wavenumber assesment was analyzed combinedly with the results of the Gaussview-5 and VEDA-4 software observations and symmetry considerations [19].

3.1. *Molecular geometry*

The chemical properties of MBMMBA were obtained using DFT at the above mentioned theory. Since the measured vibrational spectra do not contain any imaginary wavenumber, the optimized structure of the molecule MBMMBA (Fig. 1) is confirmed to be located at the local true minima on the potential energy surface.

The bond lengths, bond angles and dihedral angles of MBMMBA acquire after optimization have been compared with those reported in X-Ray crystal structure information [6] as provided in Table 1. "The geometric differences between the optimised molecule and the molecule in solid state result from the fact that the chemical conformation in the gas phase differs from that in the solid state, where intermolecular interactions play an important role in crystal structure stabilisation" [20]. The C-O bond lengths lie in the range 1.208-1.411Å which match well with the experimental values 1.275-1.428Å [6] and found nearly to the usual ester C - O lengths [21,22]. The length of

C-C bond in the phenyl ring is between 1.389 and 1.407Å, and the C-C-C bond angles are between 118.559° and 120.843°.

A clear agreement is seen in these calculated bond length, bond angles with experimental value and also those with standard bond lengths and bond angles.

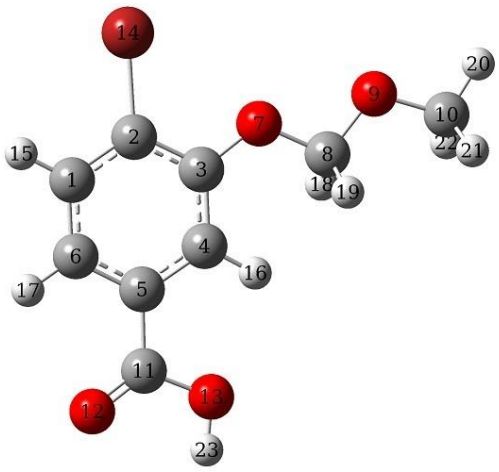

Fig. 1. Optimized structure of MBMMBA.

Table 1. The computationally optimized parameters of MBMMA and its Comparison with available experimental results [6].

Parameter	Cal. values	Exp. values	Parameter	Cal. values	Exp. values	Parameter	Cal. values	Exp. Values
Bond length(Å)			Bond angle (in degree)			Dihedral Angle (in degree)		
C1-C2	1.389	1.380	C4-C5-C11	121.448	119.4	C2-C1-C6-H17	180.0	-
C2-C3	1.407	1.400	C6-C5-C11	118.223	119.9	H15-C1-C6-C5	-180.0	-
C3-C4	1.395	1.385	C1-C6-C5	119.559	119.3	H15-C1-C6-H17	0.0	-
C4-C5	1.400	1.402	C1-C6-H17	120.945	120.4	C1-C2-C3-C4	-0.0	1.1
C5-C6	1.394	1.394	C5-C6-H17	119.495	120.4	C1-C2-C3-O7	-180.0	180.0
C6-C1	1.390	1.373	C3-O7-C8	118.774	117.7	Br14-C2-C3-C4	180.0	-176.2
C5-C11	1.485	1.476	O7-C8-O9	104.736	113.0	Br14-C2-C3-O7	-0.0	2.7
C11-O12	1.208	1.275	O7-C8-H18	110.107	109.0	C2-C3-C4-C5	0.0	0.0
C11-O13	1.359	1.271	O7-C8-H19	110.106	109.0	C2-C3-C4-H16	180.0	-
C3-O7	1.354	1.371	O9-C8-H18	111.163	109.0	O7-C3-C4-C5	180.0	-178.8
C8-O7	1.411	1.428	O9-C8-H19	111.163	109.0	O7-C3-C4-H16	0.0	-
C8-O9	1.389	1.390	H18-C8-H19	109.483	107.8	C2-C3-O7-C8	180.0	171.1
C10-O9	1.418	1.426	C8-O9-C10	112.486	113.7	C4-C3-O7-C8	-0.0	7.7
C10-H20	1.088	0.980	O9-C10-H20	106.565	109.5	C3-C4-C5-C6	0.0	-1.4
C10-H21	1.098	0.980	O9-C10-H21	111.505	109.5	C3-C4-C5-C11	-180.0	177.2
C10-H22	1.098	0.980	O9-C10-H22	111.504	109.5	H16-C4-C5-C6	-180.0	-
C8-H18	1.103	0.990	H20-C10-H21	109.089	109.5	H16-C4-C5-C11	-0.0	-
C8-H19	1.103	0.990	H20-C10-H22	109.091	109.5	C4-C5-C6-C1	-0.0	-176.9
C4-H16	1.079	0.950	H21-C10-H22	109.011	109.5	C11-C5-C6-C1	179.996	-
C6-H17	1.082	0.950	C5-C11-O12	125.037	117.5	C11-C5-C6-H17	-0.0	-
C1-H15	1.082	0.950	C5-C11-O13	113.062	117.5	C4-C5-C11-O12	-180.0	8.3
C2-Br14	1.903	1.913	O12-C11-O13	121.899	123.3	C4-C5-C11-O13	0.0	172.9
O13-H23	0.968	0.823	C11-O13-H23	106.632	124.0	C6-C5-C11-O12	0.0	170.4
Bond angle (Å)			C3-C4-H16	118.788	120.1	C6-C5-C11-O13	180.0	-8.5
C2-C1-C6	120.26	120.4	C4-C5-C6	120.327	120.6	C3-O7-C8-O9	-180.0	-

C2-C1-H15	119.28	119.8	Dihedral Angles (in degree)			C3-O7-C8-H18	60.4	-
C6-C1-H15	120.44	119.8	C6-C1-C2-C3	0.0	-0.8	C3-O7-C8-H19	-60.4	-
C1-C2-C3	120.84	121.2	C6-C1-C2-Br14	-180.0	176.5	O7-C8-O9-C10	-180.0	-
C1-C2-Br14	119.51	118.9	H15-C1-C2-C3	180.0	-	H18-C8-O9-C10	-61.1	-
C3-C2-Br14	119.64	119.9	H15-C1-C2-Br14	0.0	-	H19-C8-O9-C10	61.1	-
C2-C3-C4	118.55	118.8	C2-C1-C6-C5	0.0	0.6	C8-O9-C10-H20	180.0	-
C2-C3-O7	117.09	116.4	C8-O9-C10-H22	61.1	-	C8-O9-C10-H21	-61.0	-
C4-C3-O7	124.34	124.8	C5-C11-O13-H23	180.0	-			
C3-C4-C5	120.44	119.7	O12-C11-O13-H23	0.0	-			

3.2. *Electronic properties*

The Frontier Molecular Orbitals are vital parameters for determining the unique features of any compound. The LUMO presents the electron acceptibility property of the compound and also susceptibilty for the nucleophilic attack. Frontier orbital energy gap delivers the idea about molecular kinetic stability and chemical reactivity. By employing Gauss view program, the energy of LUMO and HOMO have been estimated, which provides the detail about energy gap between these two as 4.46 eV. The frontier orbitals 3D plots and energy gap of MBMMBA are depicted in Fig. 2. This Fig. reveals that the HOMO is spread heavily over the phenyl ring region. The high charge density is localised mainly on carboxyl group due to HOMO-LUMO transition of reflection [21]. The expansion of LUMO is almost over the whole molecule. All the HOMO and LUMO have nodes, which placed symmetrically [23,24].

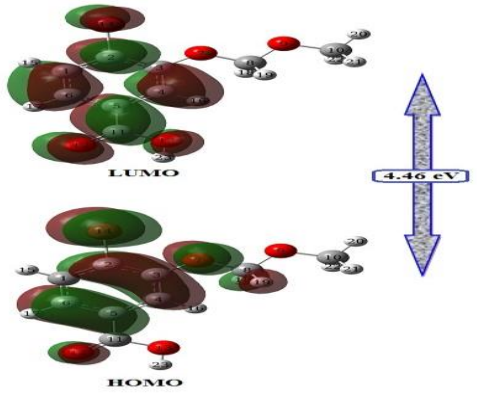

Fig. 2. Graphical presentation of band gap between FMO of MBMMBA.

The MESP surface, which is used to represent electrostatic potential and in addition to molecular shape, size is a precious mean for the exploration of connection between structure and the characteristics of substances, including biomolecules [23]. The MESP representation through color grading with mode of alignment for electrostatic potential dissipated in Fig. 3. The MESP graphic provides information about electrostatic potential of the molecule [24] and hence one can predict the sites in the molecule for electrophilic and nucleophilic attack. The MESP of the MBMMBA shows a clear variation in potential between carboxylic oxygen (dark red region in MESP, which is electronegative) and hydrogen atoms which bear most of the positive charge (green). The negative potential region surrounding the oxygen has been exhibited by the MESP plot. There are many

active electrophilic sites in the molecule whereas region near carboxylic group is more prone to active for nucleophillic attack.

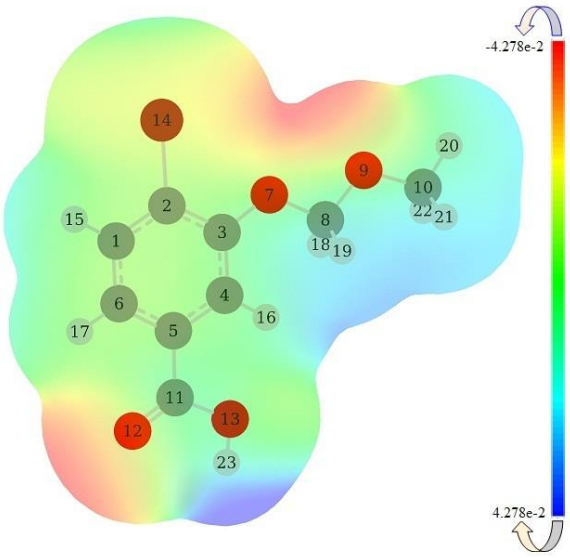

Fig. 3. MESP surface of MBMMBA.

3.3. *Vibrational analysis*

The 4-bromo-3-(methoxymethoxy) benzoic acid compound containing n (=23) atoms have (3n-6 = 63) possible fundamental vibrational modes. These modes have been elaborated and categorized as stretching (symmetric and asymmetric), scissoring, rocking, out of plane torsion modes and given in the Table 2. The vibrational frequencies have been scaled down with a factor of 0.9682 to encarporate the anharmonicity [25,26].

Table 2. Vibrational assigment of numerous modes modes of MBMMBA.

Scaled Frequency	Assignment	Scaled Frequency	Assignment
3647	ν[(O13-H23)(100)]	1196	ν[(O9-C8)(18)]+ τ_i[(H21-C10-O9-C8)(23) +(H22-C10-O9-C8)(23)]
3123	ν [(C4-H16)(99)]	1153	β [(H23-O13-C11)(29)]
3107	ν_s [(C1-H15)(30)+(C6-H17)(69)]	1139	τ_i[(H20-C10-O9-C8)(22)+(H21-C10-O9-C8)(20) + (H22-C10-O9-C8)(20)]
3093	ν_{as}[(C1-H15)(69)+ (C6-H17)(30)]	1118	ν[(C1-C6)(19)]+ β [(H17-C6-C1)(47)]
3030	ν [(C10-H22)(94)]	1109	ν_{as} [(O9-C8)(30)+ (O9-C10)(34)]
2929	ν_{as}[(C10-H21)(50)+ (C10-H22)(50)]	1105	β [(H18-C8-O9)(24)]+ τ_i[(H20-C10-O9-C8)(18) + (H18-C8-O9-C10)(31)]
2883	ν_s[(C10-H21)(47)+ (C10-H22)(47)]	1064	ν [(O13-C11)(39)]

2865	ν_{as}[(C8-H18)(50)+ (C8-H19)(50)]	1045	ν [(O7-C8)(54)]
2831	ν_s[(C8-H18)(49)+ (C8-H19)(49)]	1010	β [(C2-C1-C6)(30)]
1729	ν[(O12-C11)(83)]	995	ν_{as} [(O9-C8)(22)+ (O9-C10)(36)]
1568	ν_{as}[(C2-C1)(17)+ (C4-C3)(21)]	946	τ_i[(H15-C1-C2-C3)(34) + (H16-C4-C5-C6)(35) + (C2-C1-C6-C5)(18)]
1558	ν[(C6-C5)(38)]	917	ν [(O7-C3)(16)]
1492	β [(H19-C8-H18)(83)]	854	τi[(H16-C4-C5-C6)(54)]
1464	β [(H15-C1-C6)(25)]	819	τ_i[(H15-C1-C2-C3)(36) + (H16-C4-C5-C6)(16) + (H17-C6-C1-C2)(32)]
1455	β [(H22-C10-C21)(61)]	749	τ_o [(O12-C5-O13-C11)(60)]
1438	β [(H20-C10-H22)(38)]+ β [(H21-C10- H20)(37)]	684	τi[(C2-C1-C6-C5)(17) + (C6-C5-C4-C3)(17)]
1431	β [(H20-C10-H22)(33)]+ β [(H21-C10-H20)(33)]	641	β [(O12-C11-O13)(43) + (C6-C5-C4)(17)]
1402	τ_i [(H18-C8-O9-C10)(20)+ (H19-C8-O9-C10)(28)]	600	β [(C1-C6-C5)(26) + (C5-C4-C3)(16)]
1379	ν [(C4-C3)(17)]	579	τ_i[(H23-O13-C11-C5)(53)] + τo [(O7-C4-C2-C3)(16)]
1318	ν [(C11-C5)(17)] + β [(H23-O13-C11)(28)]	569	β [(O7-C3-C2)(29)]
1290	ν_{as} [(C2-C1)(29)+ (C4-C3)(19)+ (C5-C4)(19)]	517	τ_i[(H23-O13-C11-C5)(41) + (C2-C1-C6-C5)(16)] + τo [(O7-C4-C2-C3)(19)]
1260	β [(H16-C4-C5)(40)]	466	β [(O13-C11-C5)(48)]
1245	ν[(O7-C3)(20)]+ β [(H15-C1-C6)(24)]	433	ν[(Br14-C2)(17)]
1218	β [(H18-C8-O9)(74)]	429	τ_i[(C2-C1-C6-C5)(19) + (C6-C5-C4-C3)(20)] + τ_o [(Br14-C3-C1-C2)(20)]

C-H vibrations

C-H mode of vibrations in the form of symmetric stretching apear at frequencies 3123 cm^{-1}, 3107 cm^{-1} and 2865 cm^{-1} in this study which is in consonance with earlier reported data [27]. The bending modes involving C-H group are observed at 1464 and 1260 cm^{-1} with high intensity. The mixed modes involving C-H vibrations with variable intensities are seen at low frequecies. These modes contribute significantly in potential energy distribution (PED).

C-C vibrations

Different modes of C-C vibrations with important contributinn in PED are observed in the normal mode analysis. The asymmetric streching is found at 1568 cm^{-1} with moderate intensity. The high intesity symmetric mode is observed at 1379 cm^{-1} for C4-C3 streatching. The molecule exhibits bending of C2-C1-C6 at 1010 cm^{-1} with moderate intensity.The plane torsion modes are obseved at 946, 684 and 600 cm^{-1} having low intensity.

O-C and O-H vibrations

The O-C stretching mode is recorded at 1729 cm^{-1} with very high intensity for (O12-C11) in confirmity with value reported in litrature [28]. The asymmetric streching mode is recorded at 1110 and 1066 cm^{-1} with high intensity. Torsional mode appears at the frequency 749 cm^{-1} in title compound. Bending modes are calulated at 641 and 569 cm^{-1} at low intensities. O-C streatching contribute in mix mode of vibrations also. These modes are recorded at frequencies 1245 and 1196 cm^{-1} in present case. The symmetric stretching

mode for O13-H23 is observed at 3647 $cm^{-1}$with prominent contribution in potential energy distribution.

C-Br vibrations

C-Br streching vibrations are seen in the low frequency range at 433 and 429 cm^{-1} with good contribution in PED. The mode at the frequency 433 cm^{-1} is recognised as streching vibration of Br14-C2 with moderate intensity. Another vibration which is the torsion vibration accounted far the scaled frequency 429 cm^{-1}.

3.4. *Thermodynamic parameters*

In this section some electronic and thermodynamic parameters have been calculated through theoratical methods and represented through some specific symbols.

Table 3. Various thermodynamic parameters derived at [B3LYP/6-311++G (d,p)] level of theory.

Thermodynamic Parameter	MBMMBA
ZPE (kcal/mol)	106.05
E (kcal/mol)	115.13
C_v (cal/mol-K)	49.19
S (cal/mol-K)	123.67

ZPE (Zero point energy), thermal energy (E), entropy (S), heat capacity (C_v) for molecule MBMMBA calculated at same level. Reaction path could be facilated throuh these parameters.

3.5. *Reactivity descriptors*

Local reactivity descriptors

The atomic energy has been calculated by employing the application of Gauss View software and the reactivity parameters such as Fukui function ($f_k^{\pm}$) has been calculated for the discription. These data extract the information about reactive sites of MBMMBA. These sites are defined as neutral, electrophilic and nucleophilic sites [29]. These parameters have been calculated by following derivations[30,31]:

$$f_k^{+} = q_k(N+1) - q_k(N)$$

$$f_k^{-} = q_k(N) - q_k(N-1)$$

$$f_k^{0} = (q_k(N+1) - q_k(N-1))/2$$

Where f_k^{+}, f_k^{-} and f_k^{0} are Fukui function nucleophilic attack, electrophilic attack and radical attack respectively; and *qk*, $q_k(N+1)$, $q_k(N-1)$ is electronic population of atom *k* in neutral,anion and cation form of compound.

Table 4. Values of condensed Fukui function in MBMMBA from NBO charges in gas and aqueous phase.

ATOM	Gas Phase			Aqueous Phase		
	f_k^+	f_k^0	f_k^-	f_k^+	f_k^0	f_k^-
1C	-0.04467	-0.04877	-0.05286	-0.042	-0.01668	-0.04841
2C	-0.10738	-0.14393	-0.18047	-0.10987	-0.07955	-0.17915
3C	-0.02671	-0.01396	-0.00121	-0.02154	-0.08316	0.00234
4C	-0.07276	-0.10475	-0.13674	-0.08666	-0.06304	-0.12392
5C	-0.07738	-0.11742	-0.15745	-0.08367	-0.07519	-0.15653
6C	-0.04266	-0.15124	-0.25982	-0.06338	-0.10576	-0.26093
7O	-0.02265	-0.22239	-0.42212	-0.01941	-0.07783	-0.44412
8C	0.00213	0.081605	0.16108	0.00218	0.004445	0.16159
9O	-0.00926	-0.14928	-0.2893	-0.00459	-0.00866	-0.31917
10C	0.00229	-0.04926	-0.1008	-0.00146	-0.0007	-0.09653
11C	-0.11916	0.14456	0.40828	-0.14236	-0.06851	0.42611
12O	-0.14963	-0.24911	-0.34859	-0.16451	-0.10577	-0.3908
13O	-0.0656	-0.21081	-0.35601	-0.0708	-0.04471	-0.35111
14Br	-0.11734	-0.1286	-0.13985	-0.0783	-0.13837	-0.16537
15H	-0.02831	0.03402	0.09635	-0.02093	-0.02322	0.1027
16H	-0.02122	0.041245	0.10371	-0.02143	-0.02235	0.11042
17H	-0.02451	0.0414	0.10731	-0.02371	-0.02135	0.10593
18H	-0.00762	0.02184	0.0513	-0.00823	-0.01896	0.064
19H	-0.00761	0.02185	0.05131	-0.00823	-0.01896	0.064
20H	-0.01633	0.03557	0.08747	-0.00242	-0.00462	0.08628
21H	-0.00887	0.03211	0.07309	-0.00292	-0.00506	0.08235
22H	-0.00888	0.03211	0.0731	-0.00292	-0.00506	0.08235

In the above table (f_k^0, f_k^+,f_k^-), used to represent neutral, nucleophilic an electrophilic sites. The value of Fukui functions considering NBO charges for the respective atom of the molecule in gas and aqueous phase are tabulated in Table 4. Regarding this observation the maximum value of local reactivity descriptor f_k^+ matches to C10 atom of the molecule, it means C10 is the favorable electrophilic site and C11 is recognized as nucleophilic site according to our study. There are plenty of nucleophilic and electrophilic sites present in the molecule as revealed by the calculated data. The solvation modify the local reactivity sites and values for the molecule as also evident from the Table 4.

Global reactivity descriptors

Theoretically computed values of LUMO and HOMO serve as the foundation for estimating the compound's electron affinity and ionisation potential. According to Janak theorem and Perdew *et. al*. [32,33] ionization potential (I) and electron affinity (A) and other parameters have been derived as follows:

$I = -E_{HOMO}$ and $A = -E_{LUMO}$

$\eta = (I-A)/2$; where η represents hardness of the compound,

Chemical Potential $(\mu) = -(I+A)/2$

$S = 1/\eta$; S abbreviated as the softness of the molecules,

$\chi = (I+A)/2$; χ as electro negativity,

$\omega = \mu^2/2\eta$; ω as electrophilicity index.

The details of all global reactivity variables are listed in Table 5.

Table 5. Global reactivity descriptors for MBMMBA.

Electronic Parameter	MBMMBA
I (*eV*)	6.76
A (*eV*)	2.03
E_g (*eV*)	4.46
χ (*eV*)	4.39
η(*eV*)	2.36
μ (*au*)	3.67

3.6. *Electric moments*

The values of dipole moment (μ_{total}), polarizability (α_o) and hyperpolarizability (β) have been calculated for the compound MBMMBA and tabulated in the Table 6. The dipole moment for 4-bromo-3-(methoxymethoxy) benzoic acid has been measured as 4.0955 Debye and the polarizability presented in the Table 6 is found to be 2.1880 x 10^{-23} esu, that supports the small forntier orbital gap for MBMMBA on the basis of the discussion for 2nd perturbation theory which says that the large participation to the polarizability will be obtained from small gap between unoccupied orbitals and occupied orbitals [34]. The value of β_{total} which is abbriviation of hyperpolarizability has been measured as 9.7419 x 10^{-30} esu (50 times larger than 0.1947 x 10^{-30} esu, the hyperpolarizability value of of urea). This very high value of total Ist order static hyperpolarizability β_{total} reveals that MBMMBA molecule has good non-linear optical properties.

Table 6. Calculated value of dipole moment, polarizability and hyperpolarizability for MBMMBA.

Dipole Moment (μ_{total}) in Debye		First order static hyperpolarizability (β)	
μ_x	-0.1153	β_{xxx}	-851.4206911
μ_y	4.0883	β_{xxy}	271.0771818
μ_z	0.2145	β_{xyy}	-249.4401503
μ_{tot}	4.0955	β_{yyy}	31.7071976
Polarizability (α_o) in esu.		β_{xxz}	-0.3304575
α_{xx}	194.5268422	β_{xyz}	-0.1753489
α_{xy}	-6.96532	β_{yyz}	-0.0542168
α_{yy}	163.8507996	β_{xzz}	-12.9384306
α_{xz}	0.0004749	β_{yzz}	35.3735385
α_{yz}	0.0010543	β_{zzz}	0.0525921
α_{zz}	84.5393417	β_{total} (au)	1164.0059 au
α_o	2.1880 x 10^{-23} esu	β_{total} (esu)	9.7419 x 10^{-30}esu

5. Conclusion

The compound 4-bromo-3-(methoxymethoxy)benzoic acid ($C_9H_9BrO_4$), which belongs to the derivative of bromo–hydroxy–benzoic acids has been studied for molecular structure (bond length, bond angle), vibrational analysis, LUMO-HOMO, MESP, electronic and thermodynamic parameters and the resultant data is summerised in the form of schematic graphics and tables. The bond length and bond angle are in fair aggrement with experimental values. The energy gap between HOMO and LUMO is 4.46 eV which

shows more reactive nature of the molecule. The MESP plot of molecule indicates active electrophilic site in the molecule is over the corbon atoms whereas region near carboxylic group is prone to active for nucleophillic attack. All the vibrational modes of molecules have been calculated along with potential energy distribution. The thermal paramters of the molecule have been also calculated. The local reactivity descriptors data indicates that the most desirable site for electrophilic attack is observed at C11 and that for nucleophic and free redical attacks are found at C10 and C11 respectively; and solvation influences these sites. The hyperpolarizability has been measured as 9.7419 x 10^{-30} esu (50 times larger than that of urea) making the compoud as a good non-linear optical agent.

References

1. N. O. Anadu, V. J. Davisson, and M. Cushman, J. Med. Chem. **49,** 3897 (2006). https://doi.org/10.1021/jm0602817
2. K. Anderson, L. Wherle, M. Park, K. Nelson, L. Nguyen, and L. Salsalate, Am. Heal. Drug. Benefits **7**, 231 (2014).
3. R. Bartzatt, S. L. Cirillo, and J. D. Cirillo, Physiol. Chem. Phys. Med. NMR **36**, 85 (2004).
4. M. R. Karim, M. R. K. Sheikh, M. S. Islam, N. M. Salleh, and R. Yahya, J. Sci. Res. **11**, 383 (2019). https://doi.org/10.3329/jsr.v11i3.41578
5. Y. Bi, J. Xu, F. Sun, X. Wu, W. Ye, Y. Sun, and W. Huang, Molecules **17,** 8832 (2012). https://doi.org/10.3390/molecules17088832
6. P. A. Suchetan, V. Suneetha, S. Naveen, N. K. Lokanath, and P. K. Murthy, Acta Cryst. **E72**, 477 (2016). https://doi.org/10.1107/S2056989016003777
7. C. Hansch and T. Fujita, J. Am. Chem. Soc. **86**, 1616 (1964). https://doi.org/10.1021/ja01062a035
8. R. B. Silverman, The Organic Chemistry of Drug Design and Drug Action (Academic Press, San Diego, 1992).
9. W. Kohn and L. J. Sham, Phys. Rev. **140,** A1133 (1965). https://doi.org/10.1103/PhysRev.140.A1133
10. M. J. Frisch, et al., Gaussian 09. Revision A 02 Gaussian Inc. Wallingford CT (2009).
11. A. D. Becke, J. Chem. Phys. **98**, 5648 (1993). https://doi.org/10.1063/1.464913
12. C. Lee, W. Yang, and R. G. Parr, Phys. Rev. B **37**, 785 (1988). https://doi.org/10.1103/PhysRevB.37.785
13. B. Miehlich, A. Savin, H. Stoll, and H. Preuss, Chem. Phys. Lett. **157**, 200 (1989). https://doi.org/10.1016/0009-2614(89)87234-3
14. K. K.Yadav, A. Kumar, S. Begam, K. Nurjamal, and A. Kumar, J. Serb. Chem. Soc. **85**, 53 (2020). https://doi.org/10.2298/JSC181228102Y
15. K. K. Yadav, A. Kumar, A. Kumar, N. Misra, and G. Bramhchari, J. Mol. Struct. **1154**, 596 (2018). https://doi.org/10.1016/j.molstruc.2017.09.095
16. A. P. Scott and L. Random, J. Phys. Chem. **100**, 16502 (1996). https://doi.org/10.1021/jp960976r
17. P. Pulay, G. Fogarasi, G. Pongor, J. E. Boggs, and A. Vargha, J. Am. Chem. Soc. **105,** 7037 (1983). https://doi.org/10.1021/ja00362a005
18. Æ Frisch., H..P. Hratchian., R..D. Dennington, T.A. Keith, J. Millam, A. B. Nielsen, A. J. Holder, J. Hiscocks Gaussian, Inc. GaussView Version 5.0, June 2009.
19. M. H. Jamroz, Vibrational Energy Distribution Analysis: VEDA 4 Program Warsaw, Poland (2004).
20. A. R. Pallipurath, J. M. Skelton, A. Britton, E. A. Willneff, and S. L. M. Schroeder, Crystals **11,** 509 (2021). https://doi.org/10.3390/cryst11050509
21. K. B. Benzon, H. T. Varghese, C. Y. Panicker, K. Pradhan, B. K. Tiwary, A. K. Nanda, and C. V. Alsenoy, Spectrochim. Acta A **151**, 965 (2015). https://doi.org/10.1016/j.saa.2015.07.020

22. S. Subashchandrabose, H. Saleem, Y. Erdogdu, G. Rajarajan, and V. Thanikachalam, Spectrochim. Acta Part A **82**, 260 (2011). https://doi.org/10.1016/j.saa.2011.07.046
23. K. K. Yadav, A. Kumar, A. Kumar, G. Brahmachari, and N. Misra, Polycyclic Aromatic Compds. (2020). https://doi.org/10.1080/10406638.2020.1832126
24. R. G. Parr and W. Yang, Density Functional Theory of Atoms and Molecules (Oxford University Press, New York, 1989).
25. J. A. Pople, H. B. Schlegel, R. Krishnan, D. J. Defrees, J. S. Binkley, M. J. Frisch, R. A. Whiteside, R. F. Hout, and W. J. Hehre, Int. J. Quantum Chem. **15**, 269 (1981).
26. M. A. Plafox, Int. J. Quantum Chem. **77**, 661 (2000). https://doi.org/10.1002/(SICI)1097-461X(2000)77:3%3C661::AID-QUA7%3E3.0.CO;2-J
27. P. C. Maurya, K. K. Yadav, and A. Kumar, Biointerface Res. Appl. Chem. **9**, 4150 (2019). https://doi.org/10.33263/BRIAC94.150156
28. A. Kumar, V. Narayan, O. Prasad, and L. Sinha, J. Mol. Struct. **1022**, 81 (2012). https://doi.org/10.1016/j.molstruc.2012.04.089
29. I. Singh, A. A. El-Emam, S. K. Pathak, R. Srivastava, V. K. Shukla, O. Prasad, and L. Sinha, Mol. Simul. **45**, 1029 (2019).
30. R. G. Parr and R. G. Pearson, J. Am. Chem. Soc. **105**, 7512 (1983). https://doi.org/10.1021/ja00364a005
31. P. K. Chattaraj, H. Lee, and R. G. Parr, J. Am. Chem. Soc. **113**, 1854 (1991). https://doi.org/10.1021/ja00005a072
32. J. F. Janak, Phys. Rev. B **18**, 7165 (1978). https://doi.org/10.1103/PhysRevB.18.7165
33. J. P. Perdew, R. G. Parr, M. Levy, and L. B. Jose Jr, Phys. Rev. Lett. **49**, 1691 (1982). https://doi.org/10.1103/PhysRevLett.49.1691
34. F. Jenson, Introduction to Computational Chemistry, 2nd Edition (John Wiley and Sons Ltd., 2007).